

Novel closed-cycle reaction mode for totally green production of Cu1.8Se nanoparticles based on laser-generated Se colloidal solution

Zhangyu Gu(顾张彧)[1,2,†], Yisong Fan(范一松)[3,†], Yixing Ye(叶一星)[2,†], Yunyu Cai(蔡云雨)[2,‡], Jun Liu(刘俊)[2], Shouliang Wu(吴守良)[2], Pengfei Li(李鹏飞)[2], Junhua Hu(胡俊华)[4], Changhao Liang(梁长浩)[2,4,5,§], and Yao Ma(马垚)[2,6]

Citation: Chin. Phys. B, 2022, 31 (7): 078102 DOI: 10.1088/1674-1056/ /ac6db2
Journal homepage: http://cpb.iphy.ac.cn; http://iopscience.iop.org/cpb

What follows is a list of articles you may be interested in

SnO_2/Co_3O_4 nanofibers using double jets electrospinning as low operating temperature gas sensor

Zhao Wang(王昭), Shu-Xing Fan(范树兴), and Wei Tang(唐伟)
Chin. Phys. B, 2022, 31 (**2**): 028101. DOI: 10.1088/1674-1056/ac1336

Adsorption of CO_2 on MgAl layered double hydroxides: Effect of intercalated anion and alkaline etching time

Yan-Yan Feng(冯艳艳), Xiao-Di Niu(牛潇迪), Yong-Hui Xu (徐永辉), and Wen Yang(杨文)
Chin. Phys. B, 2021, 30 (**4**): 048101. DOI: 10.1088/1674-1056/abd750

Theoretical studies on alloying of germanene supported on Al (111) substrate

Qian-Xing Chen(陈前行), Hao Yang(杨浩), and Gang Chen(陈刚)†
Chin. Phys. B, 2020, 29 (**10**): 108103. DOI: 10.1088/1674-1056/ab9c08

Construction of monolayer $IrTe_2$ and the structural transition under low temperatures

Aiwei Wang(王爱伟), Ziyuan Liu(刘子媛), Jinbo Pan(潘金波), Qiaochu Li(李乔楚), Geng Li(李更), Qing Huan(郇庆), Shixuan Du(杜世萱), Hong-Jun Gao(高鸿钧)
Chin. Phys. B, 2020, 29 (**7**): 078102. DOI: 10.1088/1674-1056/ab90eb

Uncovering the internal structure of five-fold twinned nanowires through 3D electron diffraction mapping

Xin Fu(付新)
Chin. Phys. B, 2020, 29 (**6**): 068101. DOI: 10.1088/1674-1056/ab8370

SPECIAL TOPIC — Laser and plasma assisted synthesis of advanced nanomaterials in liquids

Novel closed-cycle reaction mode for totally green production of $Cu_{1.8}Se$ nanoparticles based on laser-generated Se colloidal solution

Zhangyu Gu(顾张彧)[1,2,†], Yisong Fan(范一松)[3,†], Yixing Ye(叶一星)[2,†], Yunyu Cai(蔡云雨)[2,‡], Jun Liu(刘俊)[2], Shouliang Wu(吴守良)[2], Pengfei Li(李鹏飞)[2], Junhua Hu(胡俊华)[4], Changhao Liang(梁长浩)[2,4,5,§], and Yao Ma(马垚)[2,6]

[1] *Henan Institute of Advanced Technology, Zhengzhou University, Zhengzhou* 450001, *China*
[2] *Key Laboratory of Materials Physics and Anhui Key Laboratory of Nanomaterials and Nanotechnology, Institute of Solid State Physics, Hefei Institutes of Physical Science, Chinese Academy of Sciences, Hefei* 230031, *China*
[3] *Anhui Institute of Optics and Fine Mechanics, Hefei Institutes of Physical Science, Chinese Academy of Sciences, Hefei* 230031, *China*
[4] *School of Materials Science and Engineering, Zhengzhou University, Zhengzhou* 450001, *China*
[5] *University of Science and Technology of China, Hefei* 230026, *China*
[6] *Technology Center, Benecke Changshun Auto Trim (Zhangjiagang) Co., Ltd., No.* 8, *Changyang Rd., Nansha, Jingang Town, Zhangjiagang* 215632, *China*

(Received 6 March 2022; revised manuscript received 3 April 2022; accepted manuscript online 7 May 2022)

Non-stoichiometric copper selenide ($Cu_{2-x}Se$, $x = 0.18 \sim 0.25$) nanomaterials have attracted extensive attentions due to their excellent thermoelectric, optoelectronic and photocatalytic performances. However, efficient production of $Cu_{2-x}Se$ nanoparticles (NPs) through a green and convenient way is still hindered by the inevitable non-environmentally friendly operations in common chemical synthesis. Herein, we initially reveal the coexistence of seleninic acid content and elemental selenium (Se) NPs in pulsed laser-generated Se colloidal solution. Consequently, we put forward firstly a closed-cycle reaction mode for totally green production of $Cu_{1.8}Se$ NPs to exclude traditional requirements of high temperature and toxic precursors by using Se colloidal solution. In such closed-cycle reaction, seleninic acid works as the initiator to oxidize copper sheet to release cuprous ions which can catalyze the disproportion of Se NPs to form SeO_3^{2-} and Se^{2-} ions and further produce $Cu_{2-x}Se$ NPs, and the by-product SeO_3^{2-} ions promote subsequent formation of cuprous from the excessive Cu sheet. In experiments, the adequate copper (Cu) sheet was simply dipped into such Se colloidal solution at 70 °C, and then the stream of $Cu_{1.8}Se$ NPs could be produced until the exhaustion of selenium source. The conversion rate of Se element reaches to more than 75% when the size of Se NPs in weakly acidic colloidal solution is limited between 1 nm and 50 nm. The laser irradiation duration shows negative correlation with the size of Se NPs and unobvious impact to the pH of the solution which both are essential to the high yield of $Cu_{1.8}Se$ NPs. Before Cu sheet is exhausted, Se colloidal solution can be successively added without influences to the product quality and the Se conversion rate. Such green methodology positively showcases a brand-new and potential strategy for mass production of $Cu_{2-x}Se$ nanomaterials.

Keywords: non-stoichiometric copper selenide, green production, selenium colloidal solution, laser irradiation in liquids

PACS: 81.07.–b, 79.20.Eb, 64.70.pv, 73.61.Le **DOI:** 10.1088/1674-1056/ac6db2

1. Introduction

As an important member of copper chalcogenide nanomaterials, $Cu_{2-x}Se$ ($x = 0.18 \sim 0.25$) is widely demanded in many fields such as solar cells,[1,2] photothermal therapy,[3–7] photoacoustic imaging,[8] thermoelectric converters[9] and so on, because it has tunable stoichiometric composition, numerous phases and morphologies. In existed reports, various synthetic methods have been explored to generate diversified $Cu_{2-x}Se$ nanomaterials with different shapes and properties.[10] For example, $Cu_{2-x}Se$ nano-cubes,[11] ultrasmall plasmonic $Cu_{2-x}Se$ particles,[5] $Cu_{2-x}Se$ nanowires,[12] and $Cu_{2-x}Se$ nanosheets with controllable thickness[13] can be obtained by the one-pot solution strategy, the ambient aqueous method, the modified composite hydroxide mediated method and the cation exchange reactions, respectively. For decades, these synthesis approaches still cannot avoid the problems from relatively toxic raw materials, air sensitive process, high temperature, and so on.[14,15] The commonly used raw selenium materials include selenium powder, selenite, and selenium dioxide.[1,12,16] Selenite and selenium dioxide both have strong toxicity of human physiology and environment. Elemental selenium powder is relatively low toxic, but it must undergo a reduction process to be an acute toxic selenide. In the above-mentioned methods, to keep the stability of the cuprous ions, some protective measures are necessary, including inert gas, reductants, organic stabilizers, and so on. Meanwhile, the temperature at which $Cu_{2-x}Se$ is formed has been reported to be between 160 °C and 250 °C,[5,10–13,17] and it is not conduc-

[†] These authors contributed equally to this work.
[‡] Corresponding author. E-mail: yycai@issp.ac.cn
[§] Corresponding author. E-mail: chliang@issp.ac.cn

© 2022 Chinese Physical Society and IOP Publishing Ltd

tive to effective toxic control of heavily used selenium source. There is still a lack of truly green and convenient synthesis strategy to obtain $Cu_{2-x}Se$ NPs, especially for mass production.

According to the synthesis principle in the above-mentioned methods, the formation of $Cu_{2-x}Se$ is on the basis of combination between Cu^+ ions and Se^{2-} ions which come from the reduction of SeO_2, SeO_3^{2-} or Se powder. The key for green production of $Cu_{2-x}Se$ NPs has been to avoid heavy using of these toxic Se precursors and avoid emerging of hazardous intermediates. It is well known that the elemental Se NPs can be used as an additive for food and drugs due to the higher bio-availability and lower toxicity than organic and inorganic forms of Se.[18] Researchers have already proved that Cu^+ ions can catalyze the disproportion of elemental Se NPs to form SeO_3^{2-} and Se^{2-} which can immediately combine with Cu^+ ions to form Cu_2Se to avert the threat from accumulated Se^{2-} ions.[19] As the copper deficient cuprous selenide, $Cu_{2-x}Se$ NPs can be originated from Cu_2Se NPs through a phase transformation promoted by air exposure and the unreacted oxidants.[20] These results indicate that Se NPs have good potential as a safe precursor for production of $Cu_{2-x}Se$. However, in such process, a constant supply of air sensitive Cu^+ ions must be provided to keep the disproportionated reaction going and the Cu_2Se forming. It means that the reactions need to take place in a strict reductive environment. What is more, partial elemental Se changes into toxic SeO_3^{2-} ions which contradict the prerequisite for the green synthesis. Interestingly, on the basis of redox potential as the measurement of the tendency of an environment to oxidize or reduce substrates,[21] H_2SeO_3 can oxidize the Cu metal to generate element Se and Cu_2O which will be dissolved into cuprous ions in acid solution. This exhibits a new idea on how to eliminate the by-product of SeO_3^{2-} ions in above disproportionated reaction and to compensate cuprous ions in solution simultaneously.

On the other hand, there is a powerful preparation of green and safe Se NPs from the low toxic Se powder by pulsed laser irradiation in liquid (PLIL) technique which has always been deemed as a special methodology compatible with the 12 principles of green chemistry for achievement of nanoparticles.[22,23] In addition, the possibility of remote control and PC control for PLIL make this technology more suitable for continuous gram-scale nanoparticle production.[24,25] Different from other synthesis methods, such as *in vivo* synthesis, direct solution-phase synthesis, and acrylonitrile-induced synthesis.[26–28] PLIL generated Se colloidal nanoparticles in deionized water possess advantages in highly purity and tunable size according to our reported articles.[29–31] To our surprise, in our experiments, PLIL generated Se NPs in colloidal solution coexist with a little of SeO_2 due to the mild oxidation so as to the formation of minor H_2SeO_3 in solution. This phenomenon has never been reported in previous reports. It indicates that PLIL generated Se colloidal solution potentially realize oxidation of Cu metal to supply cuprous ions which can catalyze Se NPs for the formation of $Cu_{2-x}Se$ NPs, and promote the recycle of the by-product SeO_3^{2-}.

Herein, we firstly verified aforementioned deductions experimentally, and creatively came up with a totally green closed-cycle reaction to conveniently acquire $Cu_{2-x}Se$ NPs with good potential for mass production. By pulsed laser irradiation in deionized water, the low toxic Se powder has been changed into safe Se NPs in order to avoid the toxic problems. Copper sheet has been chosen as a raw reactant without serious air sensitivity. Such closed-cycle reaction comprises four steps: (i) the generated H_2SeO_3 content during laser irradiation initially oxidizes copper to Cu_2O and promote the release of Cu^+ ions in acid environment; (ii) Cu^+ ions further catalyze Se NPs to form SeO_3^{2-} and Se^{2-} ions; (iii) Se^{2-} ions combine with Cu^+ ions to generate Cu_2Se which will be oxidized as $Cu_{2-x}Se$ in solution; and (iv) the by-product of SeO_3^{2-} continues to react with the rest Cu sheet for the formation more Cu^+ ions. In our experiments, the impacts from parameters of Se colloidal solutions modulated by pulsed laser and reaction temperature all had been discussed. After counting, the conversion rate from element Se to $Cu_{2-x}Se$ reached 75% for one batch of Se colloidal solution. Due to the excess of Cu sheet (1 cm^2), the volume of Se colloidal solution (100 ppm) was increased from 50 mL to 500 mL without obvious change for conversion rate of Se element. What is more, the newly formed Se colloidal solution could be added for several times to eliminate the rest Cu sheet. For the products of $Cu_{2-x}Se$ from different batches, they possessed the same phase structure, size distribution and conversion rate of Se element. All results showcase a brand-new strategy for totally green and convenient production of $Cu_{2-x}Se$ NPs with a high conversion rate of Se element and without heavy use of toxic precursors. The successive adding of Se colloidal solutions to react with excessive Cu source also shows great potential for a quasi-continuous mode of mass production of $Cu_{2-x}Se$ NPs.

2. Experimental section

2.1. Materials

Herein, the raw materials for obtaining $Cu_{1.8}Se$ NPs just comprised selenium powder (200 mesh, purity 99.99%) and copper sheets (AR, 99.5% metals basis, 0.1-mm thickness) which were both purchased from Aladdin Industrial Corporation. The deionized water used in the whole experiment was produced by a laboratory water purifier (Millipore direct-Q 5 UV).

2.2. Characterization

The images about morphology, size, crystal facets of the products were carefully observed and collected by a field-emission scanning electron microscope (FESEM, model Hitachi SU8020) and a transmission electron microscope (TEM, FEI Tecnai TF20 operated at 200 kV). X-ray diffraction (XRD) data were tested on a Philips X' Pert system with Cu K_α radiation ($\lambda = 1.5418$ Å) to investigate the crystal structure of the products synthesized. The absorption properties of the samples were recorded by UV–Vis–NIR spectrophotometer (UV3600-MPC3100 spectrophotometer). X-ray photoelectron spectroscopy (XPS, Thermo ESCALAB 250) was employed to analyze the chemical state of samples. Inductively coupled plasma mass spectrometer (ICP-MS, icap Qc) was used to determine the content of target elements in samples.

2.3. Experiments

2.3.1. PLIL synthesis of selenium colloidal solution

In this work, the pulsed laser irradiation in liquid (PLIL) technique was utilized to prepare selenium colloidal solution as the active precursor for generation of $Cu_{2-x}Se$ NPs. In detail, first, selenium powder was mixed with deionized water to form a suspension at the concentration of 100 ppm after the ultrasonic treatment. Second, such suspension (50 mL) in a glass bottle was irradiated by an Nd:YAG nanosecond pulsed laser with the assistance of the magnetic stirrer. The chosen parameters of the laser included pulse duration 7 ns, wavelength 532 nm, pulse repetition rate 50 Hz, energy per pulse 200 mJ, and output power 10 W. After irradiation for 10 min, the Se suspension transformed to Se colloidal solution, and then displayed obvious Tyndall effect indicating the existence of a large number of Se NPs. This product was labeled as Se-1. For comparation, the laser irradiation duration was changed as 5 min, 20 min, and 40 min, and such formed Se colloidal solutions were recorded as Se-2, Se-3, and Se-4, respectively. The schematic diagram of preparation process is shown in Fig. 1.

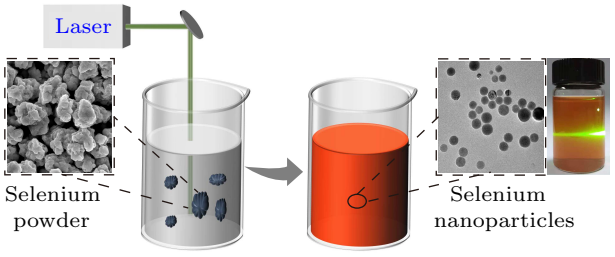


Fig. 1. Schematic diagram for preparation of Se colloidal solution by PLIL technique.

2.3.2. Closed-cycle synthesis of monodisperse $Cu_{2-x}Se$ NPs

The copper sheet (1 cm^2) was dipped in the above-mentioned Se colloidal solution at 70 °C for 48 h until the color of the solution changed from brick red to dark green indicating the exhaustion of original Se source and formation of $Cu_{2-x}Se$ NPs. After standing for 12 h, $Cu_{2-x}Se$ NPs precipitated and made the solution clean. The residual copper sheet continued to react with the newly supplied Se colloidal solution until the copper was completely used. As formed $Cu_{2-x}Se$ NPs were successfully synthesized by a closed-cycle process through a series of reactions so as to the reuse of the by-product of H_2SeO_3 and the high conversion rate of Se element. The detail of the synthesis was discussed in the following part.

3. Results and discussion

Figure 2 shows basic characterization of Se NPs in colloidal solutions generated from Se powder by pulsed laser irradiation in deionized water. In Figs. 2(a)–2(d), TEM images of Se NPs in four groups revealed the size change under different laser irradiation durations. The average sizes of Se NPs in Se-1, Se-2, Se-3, and Se-4 groups were counted as 51.51 ± 8.38 nm, 101.11 ± 46.40 nm, 15.87 ± 6.71 nm, and 1.53 ± 0.38 nm, respectively. XRD patterns in Fig. 2(e) and selected area electron diffraction (SAED) pattern inserted in Fig. 2(a) both confirmed that laser-generated Se NPs has amorphous state under different laser irradiation durations. Raman spectra for the four samples in Fig. 2(f) display a same peak at around 257 cm^{-1} which corresponds to the A_1 symmetric stretching mode of amorphous Se.[29] According to our previous reports, pulsed laser irradiation can melt bulk Se so as to generate amorphous Se NPs in liquid with variable sizes and shapes.[30,31] Herein, the chosen selenium powder has the average size of ~ 2 μm (see Fig. S1 in Supporting information), and looks like small Se bulks. When intensively heated by the absorbed laser, the powder will suffer from melting and/or evaporation in water and decomposition into smaller fragments.

In Fig. 2(g) for the sample Se-1, a doublet between 57 eV $\sim$ 54 eV with a spin orbit splitting energy of 0.86 eV was well attributed to the element Se.[32] Interestingly, a weak peak at 59 eV in Fig. 2(g) was also observed. It is well attributed to Se $3d_{5/2}$ from H_2SeO_3 indicating the existence of Se element with high valency state in solution.[33] This phenomenon was also observed for other samples (see Fig. S2). Meanwhile, in Fig. 2(h), pH values of the four Se colloidal solutions changed in a narrow range from 4.91 to 5.75 indicating a stable acidity feature after laser irradiation. ICP-MS test also confirmed the formation of the ionic Se species with low concentration in solution (see Fig. S3). Especially for Se-1 group, the proportion of oxidized Se element was calculated as about 1.6%. Therefore, it is inferred that a small amount of selenium element undergoes the oxidation change during laser irradiation. Laser irradiation can greatly reduce the size of Se particles, but has no obvious effect on pH value of Se colloidal solution.

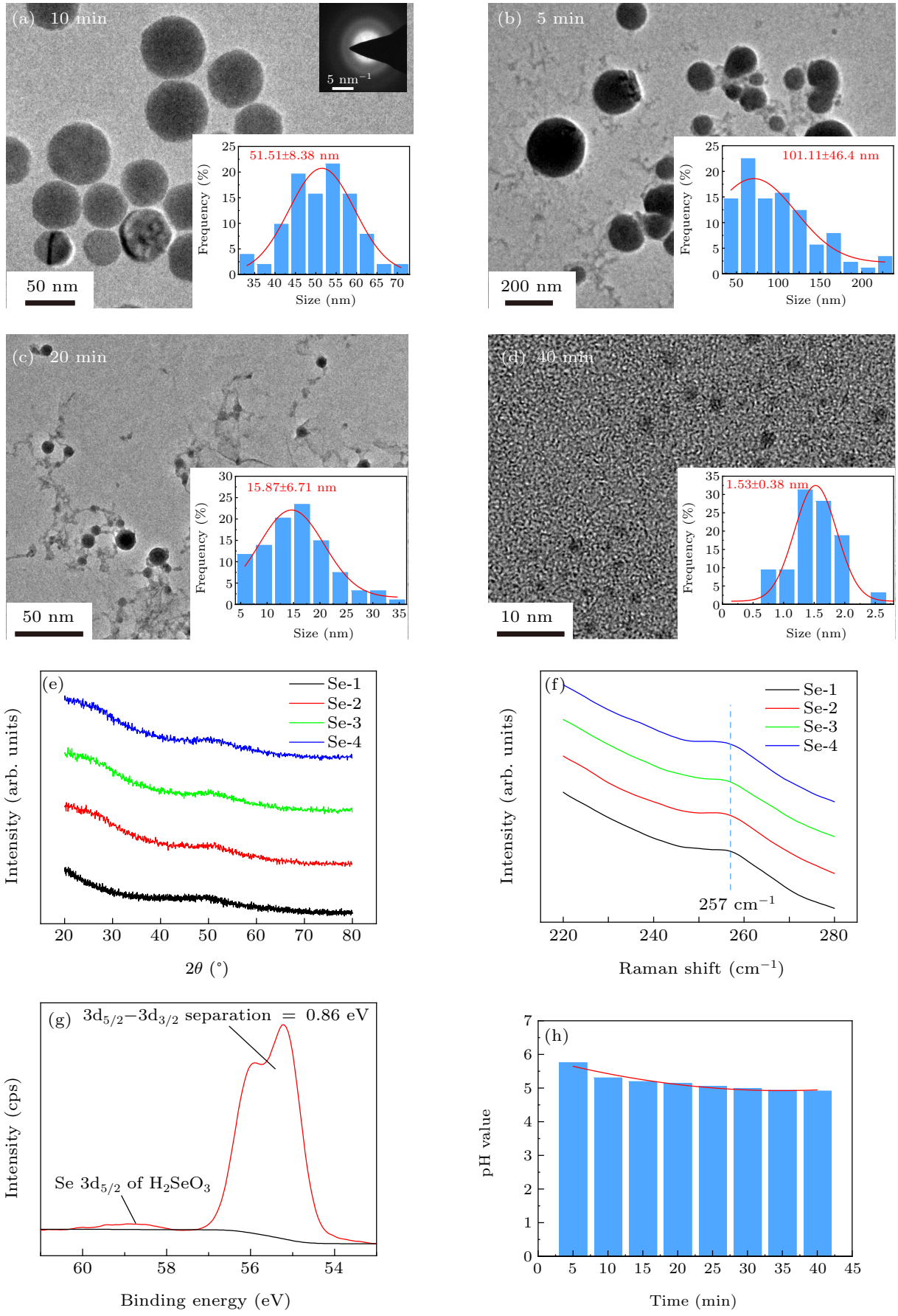


Fig. 2. The characterization of selenium colloidal solutions: (a)–(d) TEM images of Se NPs in the corresponding groups with inserted grain diameter distribution maps; (e) XRD patterns of selenium NPs; (f) Raman pattern; (g) XPS spectrum of sample; (h) relationship between pH value of Se colloidal solution and irradiation time.

Figure 3 outlines the synthesis process from dipping of copper sheet in Se colloidal solution to generation of $Cu_{2-x}Se$ NPs. In Fig. 4, the product generated by Se-1 sample and Cu sheet was analyzed. The obtained NPs possess good dispersibility in water. TEM image in Fig. 4(b) shows that these NPs are ovoid with mean size around 70 nm. The high-resolution TEM image inserted in Fig. 4(b) displays distinguishable lattice spacing of 0.33 nm corresponding to the plane (111) of berzelianite $Cu_{2-x}Se$.[3] The XRD pattern in Fig. 4(c) of the as-prepared NPs shows three diffraction peaks located at 27.75°, 46.10°, and 54.67°, assigned to the (111), (220), (311) planes of cubic berzelianite $Cu_{1.8}Se$, respectively (JCPDS No. 88-2045).[3] Excellent absorption performance in near-infrared region in Fig. 4(d) was also in line with traditional $Cu_{2-x}Se$ nanomaterials.[34] XPS in Figs. 4(e) and 4(f) identified the valence states of Cu and Se elements in the product. Cu $2p_{1/2}$ and Cu $2p_{3/2}$ peaks both can be separated into two peaks, respectively. In detail, the two strong peaks at 952 eV and 932.1 eV both were consistent with the univalent Cu^+ ion, while the two weak peaks at 953.9 eV and 933.5 eV were indexed well with the divalent Cu^{2+} ion.[35] It indicates that minor Cu^+ ions are oxidized to Cu^{2+} ions. The two weak satellite peaks at 965 eV–960 eV and 945 eV–940 eV respectively are recognized as shake-up satellite peaks of Cu 2p.[35,36] The peak at 916.9 eV in the Cu LMM spectrum as shown in Fig. S4 further proved the univalent state of Cu species in the product.[13,37] The double peaks at 55.3 eV and 54.6 eV were the typical Se 3d binding energy for lattice Se^{2-}.[38]

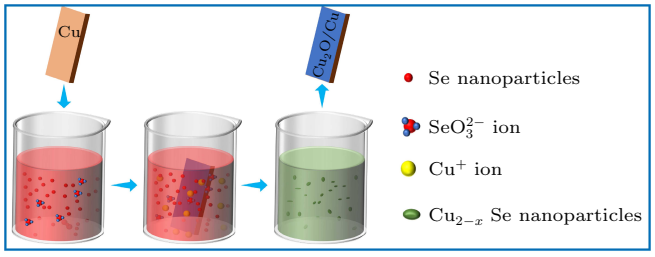


Fig. 3. Schematic diagram of synthesis of $Cu_{2-x}Se$ NPs.

To investigate the conversion of Se element, Se content before and after the reaction was compared. For Se-1 reacting with Cu sheet at 70 °C, quality ratio of Se element in final $Cu_{1.8}Se$ product to original Se powder was calculated as 75.86% by ICP-MS test in Fig. 4(b). In experiments, laser irradiation can modulate the size of Se NPs. Different Se colloidal solutions were used to react with the same Cu sheets at 70 °C, and the conversion rate of Se element was counted listed in Fig. 4(a). When the size of Se NPs was smaller than or equal to 50 nm, the conversion rate was about 75%. For Se NPs larger than 50 nm, the conversion rate decreased to about 10%. On the other hand, the effect from the reaction temperature was also analyzed. When temperature increased to 90 °C, the conversion rates for Se-1, Se-3, and Se-4 groups all rose slightly, while the conversion rate for Se-2 group dropped slightly. However, when temperature decreased to 50 °C, the conversion rate for the four groups all significantly reduced. Herein, it is reasonable to choose the optimal strategy in which Se-1 is the precursor to react with Cu sheet at 70 °C to obtain $Cu_{1.8}Se$ NPs.

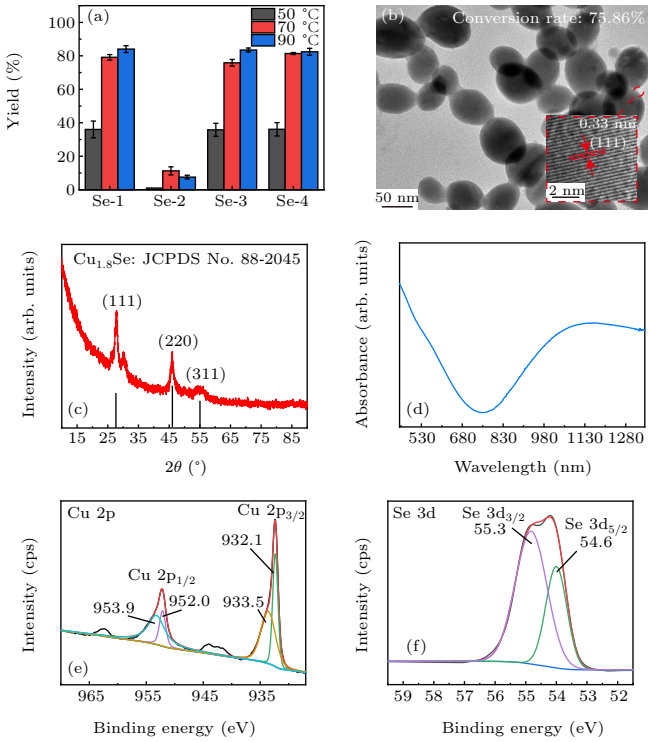


Fig. 4. (a) Comparison of production yield of $Cu_{2-x}Se$ NPs with different reaction temperatures and Se colloidal solution; (b) TEM image and HRTEM (inset image) of the as-prepared $Cu_{2-x}Se$ NPs; (c) XRD pattern; (d) UV–Vis–NIR absorbance spectra of the as-synthesized $Cu_{2-x}Se$ colloidal solution; XPS spectra of $Cu_{2-x}Se$ NPs: (e) Cu 2p; (f) Se 3d.

Figure 5 further reveals the synthesis mechanism for $Cu_{1.8}Se$ NPs. In this work, copper sheets and selenium colloidal solutions by PLIL technique are starting reactants for preparation of $Cu_{1.8}Se$ NPs. However, Se NPs in element state cannot directly react with Cu sheet because of unmatched redox potential. It is worth noting that, during the laser irradiation on Se powder, a small amount of selenium can be oxidized by oxygen in air or water to form selenium dioxide (SeO_2), which dissolves in water to form selenite (H_2SeO_3) and makes the colloidal solution acidic. As commonly reported, Cu metal can be oxidized to form Cu_2O by H_2SeO_3 in solution. It means that a thin layer of Cu_2O film can be generated on the surface of original Cu sheet in our experiments (see Eq. (1)). Due to the acidic environment, Cu^+ ions quickly dissolve from Cu sheet into the solution (see Eq. (2)). Thereafter, Cu^+ ions can make elemental Se to undergo the disproportionation catalytic reaction and convert into Cu_2Se and H_2SeO_3 species shown in Eq. (3).[19] Finally, in Eq. (4), the as-formed Cu_2Se NPs were oxidated into $Cu_{2-x}Se$ NPs through a phase transformation

promoted by air exposure and the unreacted oxidants.[20] ICP-MS results of colloids at different stages of the reaction well support this theory (Fig. S5(c) and Fig. 6(d)). In most reports, Cu^+ ions work as the initial source for $Cu_{2-x}Se$ and must be protected by reductive conditions.[5,11–13] Interestingly, because of Cu metal as the raw material in all experiments, laser induced H_2SeO_3 works as reaction initiator and reappear as the by-product which can further dissolve Cu element to introduce more and more Cu^+ ions until the Se NPs are used up. Such processes bring out a special closed-cycle reaction mechanism in our experiments.

$$H_2SeO_3 + 4Cu \rightarrow 2Cu_2O + Se + H_2O, \quad (1)$$

$$2H^+ + Cu_2O \rightarrow 2Cu^+ + H_2O, \quad (2)$$

$$4Cu^+ + 3Se + 3H_2O \rightarrow 2Cu_2Se + H_2SeO_3 + 4H^+, \quad (3)$$

$$Cu_2Se \rightarrow Cu_{2-x}Se. \quad (4)$$

Each step was monitored in our experiments to support Fig. 5 above. The morphological changes of copper sheets dipped in Se-1 solution for 12 h, 24 h, and 48 h were all observed clearly in Fig. 6(a)–6(c). From Fig. 6(a1) to Fig. 6(c1), a mass of particles located on the surface of Cu sheet and increased with the reaction duration. Such-formed particles was proved as $Cu_{1.8}Se$ NPs in Fig. 4. After removing the $Cu_{1.8}Se$ NPs, surfaces of Cu sheets in Figs. 6(a2)–6(c2) were all found to be corroded, especially for those dipped in solution more than 12 h. To investigate the intermediate products, XRD analysis was conducted and the patterns were exhibited in Fig. 6(e). The diffraction peaks at 26.76° and 44.41° can be indexed as the (111) and (220) planes of cubic $Cu_{1.8}Se$ respectively, with the lattice parameters $a = b = c = 5.765$ Å (JCPDS No. 88-2045) while the diffraction peaks at 29.55°, 36.42°, 42.30°, 61.34°, and 77.32° can be indexed as the (110), (111), (200), (220), and (222) planes of cubic Cu_2O (JCPDS No. 05-0667), respectively. Thus, it can be concluded that besides the target products (granular $Cu_{2-x}Se$ NPs) attached to the copper sheet, the residual sheet with irregular geometric polyhedrons is consist of copper and Cu_2O layer formed on the copper sheet during the reaction. Figure 6(d) also compared the Cu content in solution with and without $Cu_{1.8}Se$ NPs, and successfully proved that the dissolved Cu^+ ions participate the formation of $Cu_{1.8}Se$ NPs. We designed two experiments to identify the origin of Cu_2O layer. For one thing, the selenium colloidal solution prepared by PLIL was collected by centrifugation and redispersed in deionized water for several times to exclude H_2SeO_3 induced by laser irradiation, and then soaked the copper sheet in the newly formed solution. For another, we filtered out Se NPs from colloidal solution by the membrane to remain H_2SeO_3 content. Anther copper sheet was also soaked in the clear filtrate for comparisons. As it should be, the operations of the two experiments were completely consistent with the synthesis of $Cu_{2-x}Se$ NPs. The results were both exhibited in Figs. S5(a) and S5(b). It was found that the surface of copper sheet in the solution with only Se NPs did not change, and was covered with many Se nanoparticles (Fig. S5(b)). It was consistent with the XRD pattern showing only Cu peaks (Fig. S5(d)). Differently, for copper metal placed in the filtrate, a large number of polyhedral crystals appeared, and these polyhedral crystals were confirmed to be Cu_2O by XRD test. The ionic selenium was detected in the filtrate and copper ions were detected after copper sheet immersed in the filtrate as well. In addition, the content of copper ions rose gradually with the extension of time when the copper sheet is soaked in the filtrate (Fig. S5(c)), which further proves that H_2SeO_3 exist in Se colloidal solutions can react with copper sheets to release Cu^+. Therefore, a conclusion can be drawn that it is not the selenium element of Se NPs that oxidizes the copper surface, but the selenite existing in the solution. Cu_2O was also observed as the intermediate product of oxidation. On the other hand, Cu_2O in acidic environment would release Cu^+, which can catalyze elemental Se to Se^{2-} and SeO_3^{2-}, then Cu^+ and Se^{2-} combined rapidly to form Cu_2Se, furthermore SeO_3^{2-}could further oxidate copper sheet so as to form a closed-cycle reaction illustrated in Fig. 5.

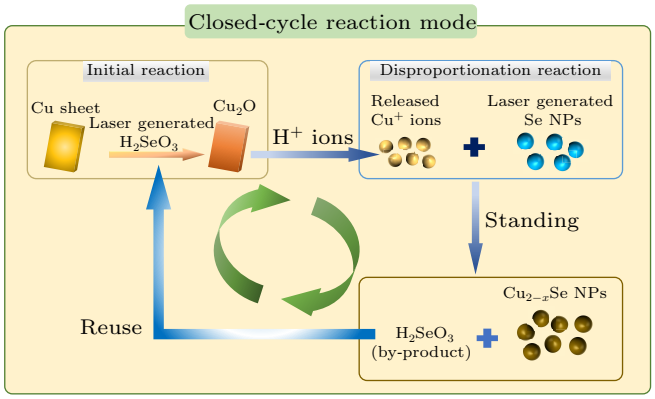


Fig. 5. Schematic diagram of the closed-cycle reaction mode.

To enhance production of $Cu_{1.8}Se$ NPs, the dose of Se-1 solution was increased from 50 mL to 500 mL. In the reaction, copper element is always excessive to Se colloid, so in theory, it is unnecessary to further increase the quality and area of the copper sheet. However, to ensure the sufficient mass and heat transfer in big vessels, we cut the copper sheets in the reaction into long strips with a width of 0.5 cm and length of 12 cm. In addition, the other reaction conditions remain unchanged. After the exhaustion of Se NPs in initial solution, the residual Cu reacted with the following supplied Se colloidal solutions for many rounds. In Fig. 7, the products generated in the first three rounds of experiments were compared. In the left column, Figs. 7(a1)–7(a3) were the photographs of Se colloidal solutions before and after reaction with Cu sheets in the first three rounds. The color changes for the three groups followed

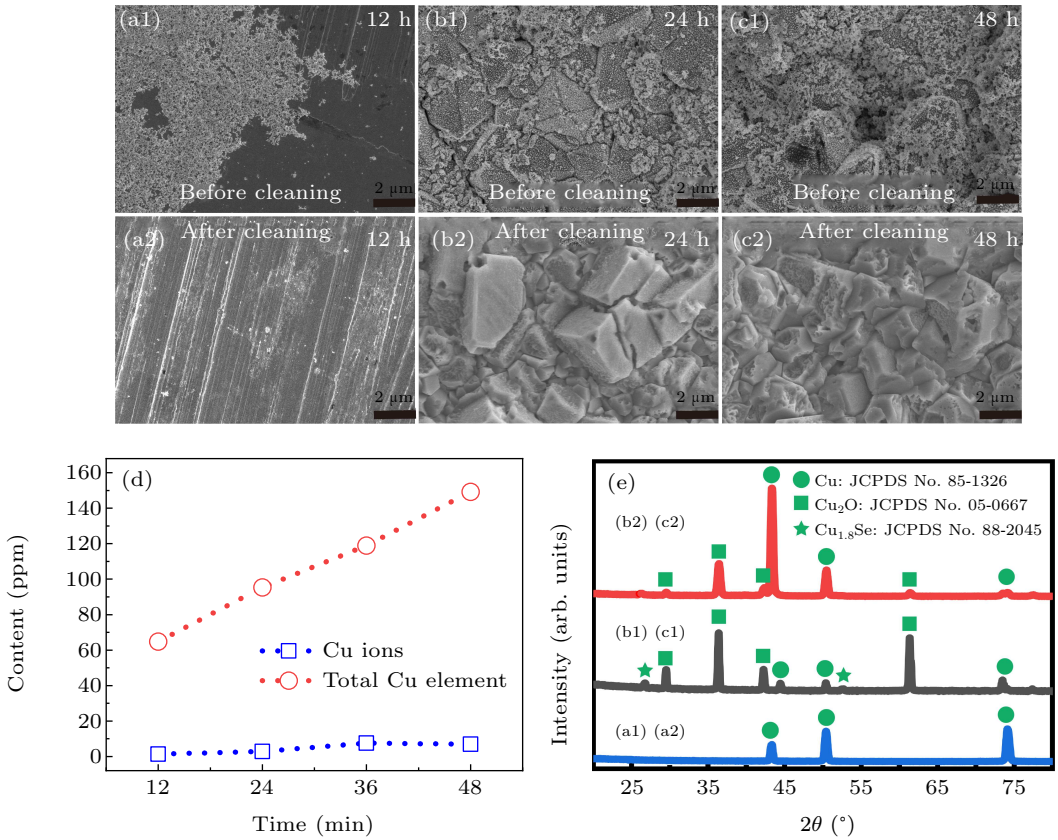


Fig. 6. Analysis of reaction intermediate processes: (a1), (b1), and (c1): SEM images of copper sheet surfaces taken from Se colloidal solution at different time (12, 24, 48 hours, respectively); (a2), (b2), and (c2): the images of the corresponding copper sheets after cleaning respectively; (d) ICP-MS results; (e) XRD patterns of the corresponding copper sheets.

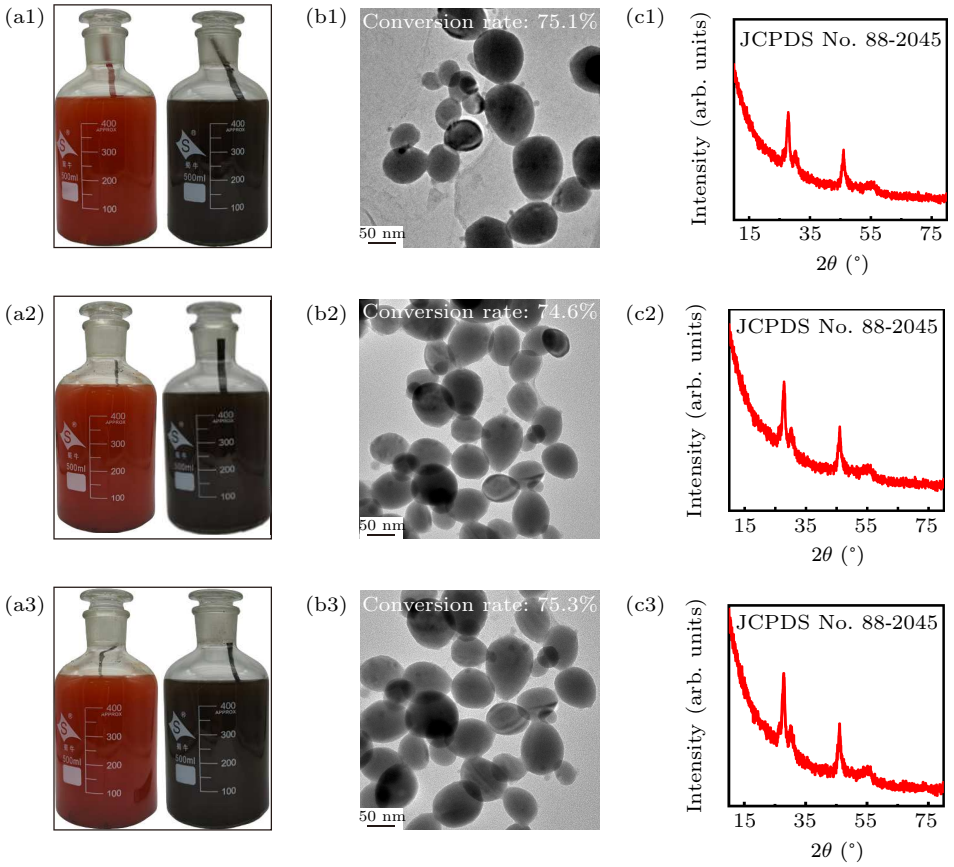


Fig. 7. (a1)–(a3) Photographs of the 500-mL large-scale synthesis in glass reaction containers corresponding to the first, second, and third batches of reactions respectively; TEM images (b1)–(b3) and XRD patterns (c1)–(c3) of products obtained in different batches.

the same pattern. For the middle column from Figs. 7(b1) to Fig. 7(b3), the average size for the products in the 3 groups located between 60 nm ∼ 70 nm, which was also similar to the result in Fig. 4(b). On the basis of ICP-MS tests, the conversion rates still reached around 75% in several times of enlarged synthesis. XRD patterns in the right column from Fig. 7(c1) to Fig. 7(c3) also confirmed the same $Cu_{1.8}Se$ phase of the three products. All data indicated that copper sheets can be used continuously without subsequent treatment to participate in the next round of synthesis and it would not make any difference to the features of the products. A reasonable explanation is that the excessive copper in the reaction makes the availability of multiple closed-cycle reaction which can be deemed as a quasi-continuous mode of production in which accumulation of toxic by-product H_2SeO_3 can be avoided and no reduction conditions is required.

4. Conclusion

In summary, we first put forward a green and convenient synthesis of $Cu_{2-x}Se$ NPs in the way of closed-cycle reaction which can be scaled up as a quasi-continuous mode of production. The copper sheets worked as the raw source to avoid the requirements for reductive conditions. Se colloidal solution generated by pulsed laser irradiation in water contains a large amount of Se NPs and a little of H_2SeO_3 as the initiator for the closed-cycle reaction. The final product was confirmed as $Cu_{1.8}Se$ NPs with average size of 70 nm. The conversion rate of Se element from Se powder to $Cu_{1.8}Se$ NPs was calculated as about 75%. In the extended experiment, the volume of the Se colloidal solution was increased to 500 mL. After several time of continues reaction with the same Cu sheet, the products were still $Cu_{1.8}Se$ NPs with unchanged size feature and Se conversion rate. Interestingly, compared with common preparation methods for $Cu_{2-x}Se$, the dose of H_2SeO_3 in this cycle-closed reaction is at a much lower level, while H_2SeO_3 as the subsequent by-product is also reused. This indicates a brand-new way to improve yield of $Cu_{2-x}Se$ products and avoid non-environmentally friendly operations on the synthesis.

Acknowledgments

Project supported by the Fund from Hefei National Laboratory for Physical Sciences at the Microscale (Grant No. KF2020110), the Natural Science Foundation of Anhui Province, China (Grant No. 1908085ME146), the Key Research and Development Plan of Anhui Province, China (Grant No. 201904a05020049), the Director Fund of Institute of Solid State Physics, Chinese Academy of Sciences (Grant No. 2019DFY01), the National Natural Science Foundation of China (Grant Nos. 52071313 and 51971211), and the Hefei Institutes of Physical Science, Chinese Academy of Sciences Director's Fund (Grant Nos. YZJJZX202018 and YZJJ202102).

References

[1] Xu J, Yang Q, Kang W, Huang X, Wu C, Wang L, Luo L, Zhang W and Lee C-S 2015 *Part. Part. Syst. Charact.* **32** 840
[2] Zhang H, Wang C, Peng W, Yang C and Zhong X 2016 *Nano Energy* **23** 60
[3] Wang X, Miao Z, Ma Y, Chen H, Qian H and Zha Z 2017 *Nanoscale* **9** 14512
[4] Wang X, Ma Y, Chen H, Wu X, Qian H, Yang X and Zha Z 2017 *Colloid. Surf. B* **152** 449
[5] Zhang S, Sun C, Zeng J, Sun Q, Wang G, Wang Y, Wu Y, Dou S, Gao M and Li Z 2016 *Adv. Mater.* **28** 8927
[6] Hu J, Song G, Han L, Zou W, Xiao Z, Huang X, Qin Z and Zou R 2014 *Nano-Micro. Lett.* **6** 169
[7] Wang X, Zhong X, Lei H, Geng Y, Zhao Q, Gong F, Yang Z, Dong Z, Liu Z and Cheng L 2019 *Chem. Mater.* **31** 6174
[8] Liu X, Lee C, Law W C, Zhu D, Liu M, Jeon M, Kim J, Prasad P N, Kim C and Swihart M T 2013 *Nano. Lett.* **13** 4333
[9] Xiao X X, Xie W J, Tang X F and Zhang Q J 2011 *Chin. Phys. B* **20** 087201
[10] Wang X, Ma Y, Sheng X, Wang Y and Xu H 2018 *Nano. Lett.* **18** 2217
[11] Xiao G, Ning J, Liu Z, Sui Y, Wang Y, Dong Q, Tian W, Liu B, Zou G and Zou B 2012 *Crystengcomm* **14** 2139
[12] Zhang Y, Hu C, Zheng C, Xi Y and Wan B 2010 *J. Phys. Chem. C* **114** 14849
[13] Wang Y, Zhukovskyi M, Tongying P, Tian Y and Kuno M 2014 *J. Phys. Chem. Lett.* **5** 3608
[14] Chen X, Gu L, Liu L, Chen H, Li J, Liu C and Zhou P 2020 *Chin. Phys. B* **29** 097201
[15] Wang A, Liu Z, Pan J, Li Q, Li G, Huan Q, Du S and Gao H J 2020 *Chin. Phys. B* **29** 078102
[16] Koren B, Friedman O, Maman N, Hayun S, Ezersky V and Golan Y 2022 *RSC. Adv.* **12** 277
[17] Chen J Y, Zhao X Y, Liu L and Xu J P 2019 *Chin. Phys. B* **28** 128101
[18] Hosnedlova B, Kepinska M, Skalickova S, Fernandez C, Ruttkay-Nedecky B, Peng Q, Baron M, Melcova M, Opatrilova R, Zidkova J, Bjorklund G, Sochor J and Kizek R 2018 *Int. J. Nanomed.* **13** 2107
[19] Lie S Q, Wang D M, Gao M X and Huang C Z 2014 *Nanoscale* **6** 10289
[20] Riha S C, Johnson D C and Prieto A L 2011 *J. Am. Chem. Soc.* **133** 1383
[21] Haynes W M, Lide D R and Bruno T J 2016 *CRC Handbook of Chemistry and Physics*, 97th edn. (CRC Press) pp. 5–75
[22] Amendola V, Amans D, Ishikawa Y, Koshizaki N, Scire S, Compagnini G, Reichenberger S and Barcikowski S 2020 *Chemistry* **26** 9206
[23] Zamiri R, Bahari-Poor H R, Zakaria A, Jorfi R, Zamiri G, Rebelo A and Omar A A 2013 *Chin. Phys. Lett.* **30** 118103
[24] Crivellaro S, Guadagnini A, Arboleda D M, Schinca D and Amendola V 2019 *Rev. Sci. Instrum.* **90** 033902
[25] Labusch M, Cunha A P, Wirtz S F, Reichenberger S, Cleve E, Söffker D and Barcikowski S 2019 *Appl. Surf. Sci.* **479** 887
[26] Cui Y H, Li L L, Zhou N Q, Liu J H, Huang Q, Wang H J, Tian J and Yu H Q 2016 *Enzyme Microb. Technol.* **95** 185
[27] Yan S, Wang H, Zhang Y, Li S and Xiao Z 2009 *Mater. Chem. Phys.* **114** 300
[28] P C, Shah, Kumar M, Pushpa K K and Bajaj P N 2008 *Cryst. Growth Des.* **8** 6
[29] Cai Y, Zhang Y, Ji S, Ye Y, Wu S, Liu J, Chen S and Liang C 2020 *J. Colloid. Interface. Sci.* **566** 284
[30] Cai Y, Ye Y, Li P, Zhou Y, Liu J, Tian Z, Yang Z and Liang C 2019 *Appl. Surf. Sci.* **473** 564
[31] Chen Q, Zhang C, Liu J, Ye Y, Li P and Liang C 2019 *Appl. Surf. Sci.* **466** 1000
[32] Shevchik N J, Cardona M and Tejeda J 1973 *Phys. Rev. B* **8** 2833
[33] Malmsten G, Thorh S H I, Bergmark J E and Karlsson S E 1971 *Phys. Scripta* **3** 96
[34] Gan X Y, Keller E L, Warkentin C L, Crawford S E, Frontiera R R and Millstone J E 2019 *Nano. Lett.* **19** 2384
[35] Yang D, Zhu Q, Chen C, Liu H, Liu Z, Zhao Z, Zhang X, Liu S and Han B 2019 *Nat. Commun.* **10** 677
[36] Brisk M A and Baker A 1975 *J. Electron Spectrosc. Relat. Phenom.* **7** 197
[37] White S L, Smith J G, Behl M and Jain P K 2013 *Nat. Commun.* **4** 2933
[38] Liu Y, Dong Q, Wei H, Ning Y, Sun H, Tian W, Zhang H and Yang B 2011 *J. Phys. Chem. C* **115** 9909